Table II
Relationship of the Critical Ethylene Sequence Length to Sample Pretreatment Temperature and the Melting Points of Simple Alkanes

copolymer	n'	T,[a] K	ref
α-olefins	12	310	8
4-methyl-1-pentene	9–13	310	this study
1-butene	6–9	298	4
α-olefins	7	253	6
vinyl chloride	3.5	223	13
1-butene	5	113	7
alkanes			
n-octadecane	8	301	
n-hexadecane	7	291	
octane	3	216	

[a] The starting temperature for the DSC run.

n' values with corresponding minimum temperatures for the DSC measurement, together with the melting points of simple hydrocarbons which may be considered as guides to the thermal stability of small PE crystallites. The general trend is clear. The observed n' value decreases with lowering of the DSC starting temperature. This presumably arises since the very small crystallites arising from short sequence lengths will be unstable at slightly higher temperatures and hence will not contribute to the observed heat of fusion.

The comparison with the alkene models is striking. Thus the data for octadecane suggests that ethylene sequence lengths of eight units will only form stable crystallites at temperatures below 301 K. The prediction appears to correspond approximately to the situation presented here, since for the copolymers studied at 310 K and above, only sequence lengths >8 are observed. It is also worthy of note that the observed values of n' for the olefin copolymers are in the range 6–13, which is of the same order of magnitude as the range 8–15 observed by authors using IR[14] and melting point data[15,16] in studies of propylene copolymers. The significantly lower values observed for the vinyl chloride copolymers might be related to additional stabilization brought about by the more rigid chain structure of the comonomer, as evidenced by higher T_g values.

Registry No. (1-Butene)(ethylene) (copolymer), 25087-34-7; (1-butene)(ethylene)(1-hexene) (copolymer), 60785-11-7; (1-decene)(ethylene)(1-octene) (copolymer), 110661-50-2; (1-butene)(ethylene)(propylene) (copolymer), 25895-47-0; (ethylene)(4-methyl-1-pentene) (copolymer), 25213-96-1; (ethylene)(vinyl chloride) (copolymer), 25037-78-9.

References and Notes

(1) Flory, P. J. *Trans Faraday Soc.* **1955**, *51*, 848.
(2) Baltá Calleja, F. J.; Rueda, D. R. *Polym. J.* (Tokyo) **1974**, *6*, 216.
(3) Glenz, W.; Kilian, H. G.; Klattenhoff, D.; Stracke, Fr. *Polymer* **1977**, *18*, 685.
(4) Kimura, K.; Shigemura, T.; Yuasa, S. *J. Appl. Polym. Sci.* **1984**, *29*, 3161.
(5) Mathot, V. B. F. *Polycon '84 LLDPE*; The plastics and Rubber Institute: London, 1984; pp 1–18.
(6) Seppala, J. V. *J. Appl. Polym. Sci.* **1985**, *30*, 3545.
(7) Krigas, T. M.; Carella, J. M.; Struglinski, M. J.; Crist, B.; Graessley, W. W.; Schilling, F. C. *J. Polym. Sci., Polym. Phys. Ed.* **1985**, *23*, 509.
(8) Burfield, D. R.; Kashiwa, N. *Makromol. Chem.* **1985**, *186*, 2657.
(9) Gan, S. N.; Burfield, D. R.; Soga, K. *Macromolecules* **1985**, *18*, 2684.
(10) Bowmer, T. N.; Tonelli, A. E. *Polymer* **1985**, *26*, 1195.
(11) Burfield, D. R.; Tait, P. J. T., unpublished results.
(12) Schilling, F. C.; Tonelli, A. E.; Valenciano, M. *Macromolecules* **1985**, *18*, 356.
(13) Bowmer, T. N.; Tonelli, A. E. *J. Polym. Sci., Polym. Phys. Ed.* **1986**, *24*, 1631.
(14) Natta, G.; Mazzanti, G.; Valvassori, G.; Sartori, G.; Morero, D. *Chim. Ind. (Milan)* **1960**, *42*, 125.
(15) Kilian, H. G. *Kolloid-Z.* **1963**, *189*, 23.
(16) Jackson, J. F. *J. Polym. Sci., Part A* **1963**, *1*, 2119.

Thermal Properties of Poly(ethylene oxide) Complexed with NaSCN and KSCN

C. Robitaille, S. Marques, D. Boils, and J. Prud'homme*

Department of Chemistry, University of Montreal, Montreal, Quebec, Canada H3C 3V1.

Received April 24, 1987; Revised Manuscript Received July 10, 1987

ABSTRACT: The melting behavior of series of solvent-cast mixtures of a low molecular weight ($\bar{M}_n = 4 \times 10^3$) poly(ethylene oxide) (PEO) with NaSCN and KSCN has been studied by DSC and optical microscopy. The results show great similarities between the two systems. Their common characteristics are first the formation of a single solid compound, P(EO_3·NaSCN) and P($EO_{\sim 4}$·KSCN), that melts incongruently to yield the solid salt and a peritectic liquid and second a liquid–liquid miscibility gap occurring at the melting point of the pure salt. Both systems exhibit a nearly vertical salt liquidus curve, indicating that complex formation also takes place in the liquid phase. The stoichiometry of the solvate is close to 4/1 for NaSCN and 5/1 for KSCN. The mixtures with NaSCN were highly crystalline over the whole composition range while those with KSCN showed either partial crystallinity or the absence of crystallinity at PEO contents above that of the solid compound. Because of the peritectic reaction, in either system the solid compound cannot participate in the formation of a eutectic mixture with the solid salt. In turn, it can form a eutectic mixture with solid PEO. In the case of the PEO–NaSCN system for which the construction of a complete phase diagram was possible, the eutectic composition is close to 93% by weight in PEO with a corresponding tie line located 4 °C below the melting point of pure PEO. The analysis of the P(EO_3·NaSCN) liquidus curve in terms of the Flory–Huggins thermodynamic concepts indicates the presence of a strong exothermic interaction ($\chi = -1.2$), associated with the solvation of P(EO_3·NaSCN) by PEO yielding the solvate P(EO_4·NaSCN). For either system, the reverse path of the peritectic reaction is not quantitative for a mixture having the composition of the solid compound. In either case, melt recrystallization yields a material that contains the solid salt in addition to the solid compound.

Introduction

Poly(ethylene oxide) (PEO) is known to form crystalline ionic complexes with several inorganic compounds, including mercuric halides,[1,2] ammonium salts,[3] and alkali-metal salts.[3-8] In the last 10 years, a great deal of interest has been generated for the ionic complexes of PEO with

0024-9297/87/2220-3023$01.50/0

alkali-metal salts because of their potential utilization as solid electrolytes for battery applications.[4] In spite of the large amount of data already published on the ionic conductivity–temperature relationships of many of these systems,[3-8] little is known concerning their phase diagrams. Several of these systems appear to yield highly as materials whose melting points depend upon the nature of the salt and its concentration. For instance, Wright[3] reported melting temperatures of 70, 100, and 195 °C, for solid mixtures of a high molecular weight PEO ($M = 4 \times 10^6$) with NH_4SCN, KSCN, and NaSCN, respectively, all being prepared by solvent evaporation from methanol solutions consisting of 4 mol of EO monomer units for 1 mol of salt. In his work, Wright assumed that, like $HgCl_2$, these three salts react with PEO to form crystalline compounds of the type $P(EO_4{\cdot}salt)$ each involving an apparent coordination number of 4 for the alkali-metal ion. More recently, Hibma[9] reported experimental evidence based upon DSC and X-ray diffraction measurements indicating a 3/1 stoichiometry for the PEO crystalline compound with NaSCN and a 4/1 stoichiometry for the compound with KSCN. In both cases the formation of a single compound was confirmed by X-ray diffraction measurements carried out on a series of mixtures of different compositions. This behavior is not general since, as shown by one of us in a recent paper[10] devoted to PEO mixtures with lithium salts, more than one crystalline compound of well-defined stoichiometry can form in some systems. For instance, this is the case for the systems PEO–$LiClO_4$ and PEO–$LiAsF_6$ which both give rise to the formation of compounds having 6/1 and 3/1 stoichiometries.

In the present paper, we describe a calorimetric study together with a thermodynamic analysis of the first-order transitions (fusion and dissolution phenomena) observed upon heating PEO–NaSCN mixtures of various compositions. A complete phase diagram of the PEO–NaSCN system was constructed in which the phase boundaries were defined by DSC measurements in conjunction with visual observations made with a polarizing microscope. Particular attention was paid to the reversibility of the phase equilibria depicted in the phase diagram. For that purpose, the mixtures were first studied as cast from methanol solutions and thereafter submitted to melt recrystallization under slow and rapid cooling conditions. Also described in the present paper is the thermal behavior of PEO–KSCN mixtures which show great similarities to the PEO–NaSCN mixtures but reveal a crystallinity gap in the domain of the PEO-rich compositions. In order to minimize entanglement effects upon the crystallinity of the specimens, a low molecular weight monodisperse PEO sample ($\bar{M}_n = 4 \times 10^3$) was used for the present study.

In a recent paper by Lee and Crist[11] some features of the phase diagram of a PEO–NaSCN system involving a high molecular weight PEO component are reported. Among these features is the presence of a PEO-rich eutectic mixture having a degree of crystallinity of 62% only. It is not clear whether this low crystallinity of the eutectic mixture was due to an entanglement effect, resulted from the annealing at 130 °C they made on the mixtures prior to their study, or was due to both these effects. Nevertheless, such a low crystallinity could seriously bias any attempt to define the stoichiometry of the crystalline compound from the composition at which the last trace of crystalline eutectic disappears in the mixtures. It might be for that reason that the 3.5/1 stoichiometry so defined by Lee and Crist is in disagreement with the 3/1 stoichiometry previously reported by Hibma.[9] We believe that the present study should clarify this point.

Experimental Section

Materials. The PEO sample (Dow Chemical Co. Polyglycol E-4000, lot number C-151) was purified by precipitation in petroleum ether from a 5% methanol solution and was subsequently dried at 70 °C under high vacuum. Its number-average molecular weight, $\bar{M}_n$, determined by vapor pressure osmometry in benzene was 3.9×10^3. Its polydispersity index, $\bar{M}_w/\bar{M}_n$, characterized by gel permeation chromatography with ultrastyragel columns in tetrahydrofurane was close to 1.01. NaSCN (Anachemia Chemical Co., reagent grade) was purified by recrystallization in distilled water and dried at 190 °C under vacuum. KSCN (Fisher Scientific Co., certified A.C.S. grade) was recrystallized in methanol and dried at 150 °C under vacuum. PEO–NaSCN and PEO–KSCN mixtures of various compositions were prepared by mixing weighted quantities of 5% methanol solutions of each component and by evaporating methanol in a chamber flushed by dry nitrogen. The solid mixtures were subsequently dried for a week under high vacuum and stored in a glovebox. Methanol (Anachemia, reagent grade) was carefully dried before utilization.

DSC Measurements. Heating and cooling curves were recorded at various rates with either a Model DSC-IB or a Model DSC-4 Perkin-Elmer calorimeter flushed with dry helium. Sample pans were filled and sealed under a dry atmosphere. Temperature calibrations were made for both instruments by using standard materials with melting points in the range −39 to 327 °C. Energy calibrations were made by using the melting peak of indium recorded at 10 °C/min.

Optical Microscopy. Optical observations were made with a Zeiss polarizing microscope equipped with a Reichert hot stage. Samples were placed between glass plates heated at about 5 °C/min. Temperature was read by means of a thermocouple fixed to one of the glass plates.

Results and Discussion

PEO–NaSCN System. As-Cast Mixtures. Figure 1 shows DSC heating curves measured at 10 °C/min on a series of as-cast PEO–NaSCN mixtures having EO/Na molar ratios ranging from 1 to 16. Also shown in Figure 1 are the DSC melting curves of the pure components. The thermal events observed in the DSC curves of Figure 1 are essentially endothermic peaks that can be attributed to either fusion or dissolution phenomena. These peaks occur in the temperature interval between 58 and 309 °C. DSC heating curves recorded at lower temperatures, from −100 °C to the range shown in Figure 1, did not exhibit any glass transition anomaly, indicating that the as-cast PEO–NaSCN mixtures were all highly crystalline at room temperature.

Inspection of the DSC curves in Figure 1 reveals the presence, over the composition range investigated, of three distinct invariant transitions that appear in the form of sharp endotherms at 58, 182, and 309 °C, respectively. The invariant transition at 58 °C occurs for all the mixtures having EO/Na ratios greater than 3. It is located 4 °C below the melting endotherm (at 62 °C) of the pure PEO component. The same mixtures (EO/Na > 3) also exhibit a second and broader endotherm at higher temperatures that increases in relative intensity and moves from 93 to 186 °C with decreasing EO/Na ratio from 16 to 3.3. For EO/Na = 3, the endotherm at 58 °C vanishes and a sharp endotherm is observed at 187 °C. Such thermal behavior is consistent with a eutectic melting at 58 °C followed by the dissolution of a crystalline compound of 3/1 stoichiometry, hereafter designated as $P(EO_3{\cdot}NaSCN)$.

The second invariant transition at 182 °C is observed for all the remaining mixtures (EO/Na < 3). As it will be shown shortly, it corresponds to an incongruent melting of the compound $P(EO_3{\cdot}NaSCN)$. Among these latter mixtures, only those with EO/Na ≤ 2 exhibit the third invariant transition at 309 °C. This latter transition co-

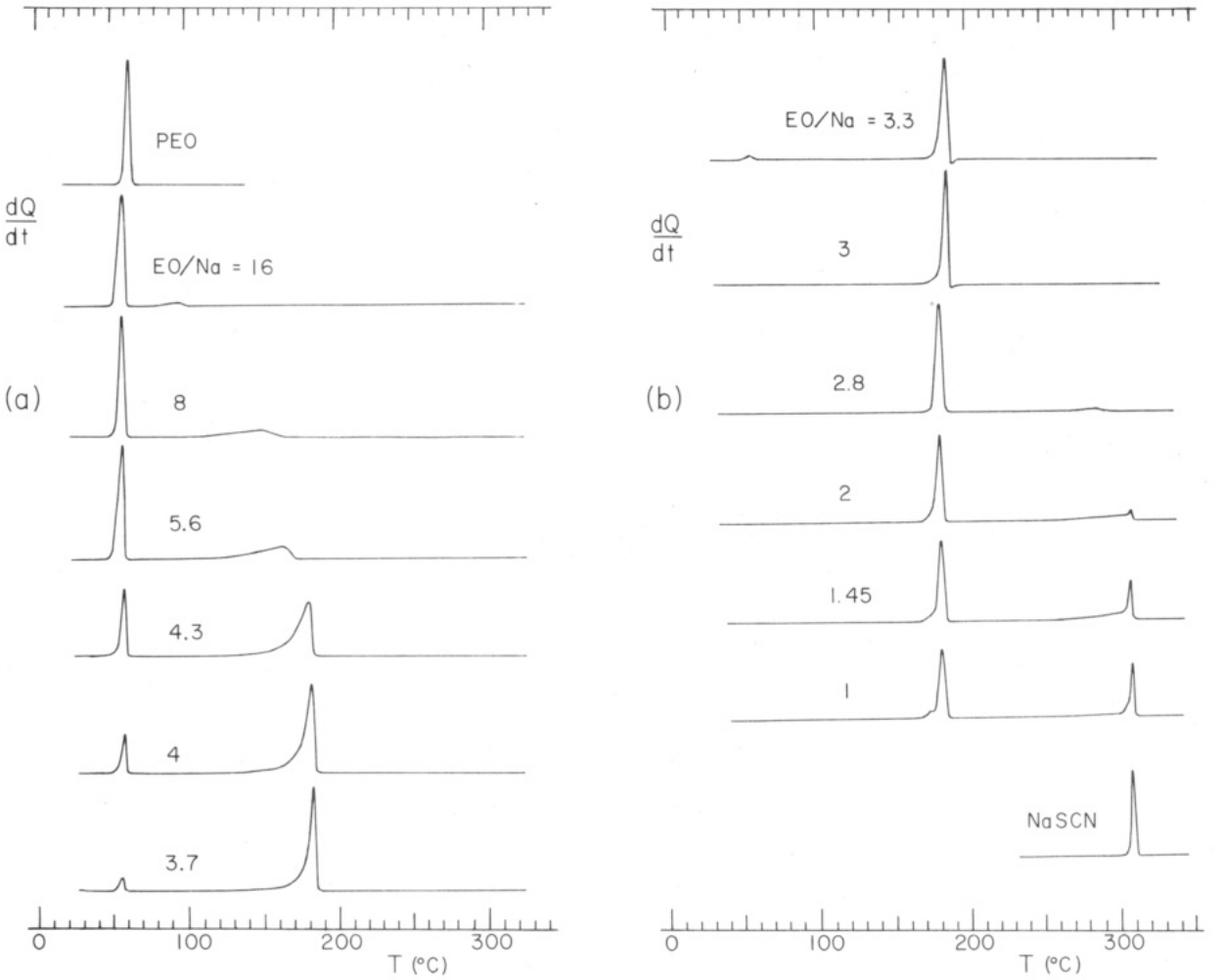

Figure 1. DSC heating curves recorded at 10 °C/min for the pure components PEO and NaSCN and for PEO–NaSCN mixtures with various EO/Na molar ratios as indicated. All samples are solvent cast from methanol solutions except NaSCN.

incides with the melting endotherm of pure NaSCN, indicating that this salt is not completely miscible with PEO over the whole range of composition.

When observed with a polarizing microscope on a hot stage heated at about 5 °C/min, the mixtures with EO/Na < 3 all exhibited a partial melting near 182 °C with a simultaneous growing of birefringent crystals within the liquid phase formed. As illustrated on Figure 2a for the mixture with EO/Na = 2, these crystals, of rhombohedral form, could reach sizes as large as 0.03 mm, indicating that they were NaSCN crystals. The granular clusters surrounding these crystals correspond to the excess of NaSCN already present in the mixture prior to its melting at 182 °C. A myriad of smaller NaSCN crystals also grew on the surface of these clusters. From these observations it is clear that the compound $P(EO_3{\cdot}NaSCN)$ undergoes an incongruent melting at 182 °C in which it disproportionates into solid NaSCN and a PEO–NaSCN liquid mixture.

Growing of NaSCN crystals was also observed at a somewhat higher temperature (185–187 °C) during the melting of the mixtures having EO/Na ratios of 3, 3.3, and 3.7. As shown on Figure 2b for the mixture with EO/Na = 3.3, there was no NaSCN granular cluster in these latter mixtures and the size of their rhombohedral crystals was much larger than for the preceding mixtures. On the other hand, once formed at either 182 or 185–187 °C, the rhombohedral crystals remained unaltered with increasing temperature up to about 240 °C and then they slowly dissolved upon further heating. No NaSCN crystal was

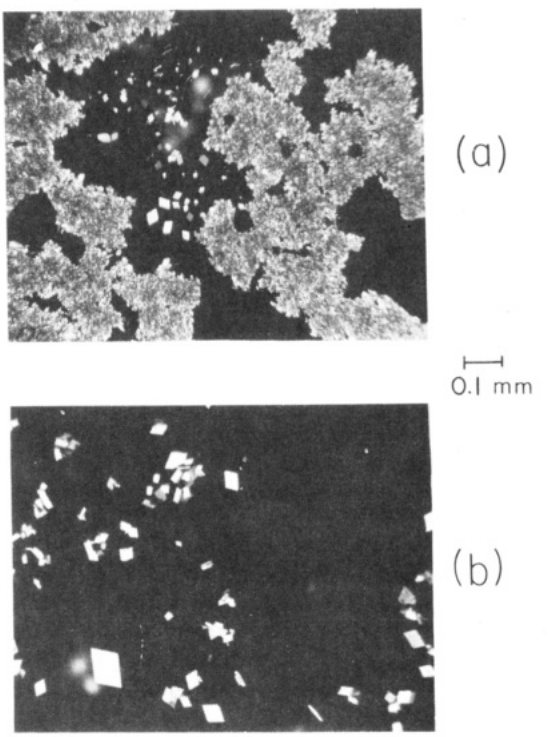

Figure 2. Photomicrographs taken at 190 °C upon the first heating of PEO–NaSCN mixtures with EO/Na = 2 (a) and EO/Na = 3.3 (b). The dark areas correspond to the peritectic liquid.

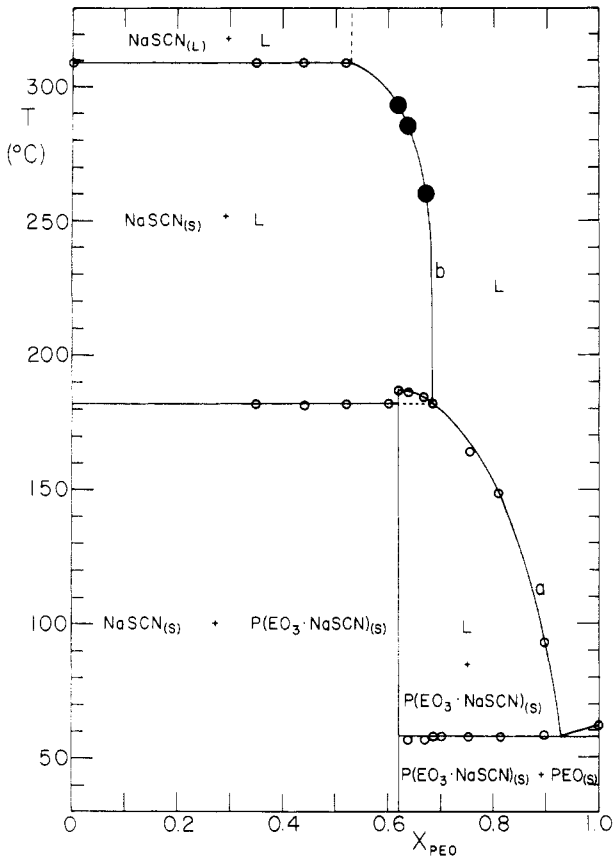

Figure 3. Temperature–composition diagram of the PEO–NaSCN system depicting the peak positions of the fusion and dissolution endotherms recorded at 10 °C/min upon the first heating of the samples. Also included are three data points (filled circles) based on optical observations indicating the dissolution end of the NaSCN crystals. The P(EO_3·NaSCN) and NaSCN liquidus curves are indicated by letters a and b, respectively. The composition is given in weight fraction of PEO, X_{PEO}.

observed for the mixtures with EO/Na ≥ 4.

Figure 3 shows a temperature–composition diagram of the PEO–NaSCN system based on the peak positions of the endotherms depicted in Figure 1. The composition is given in weight fraction of PEO designated by X_{PEO}. This temperature–composition diagram also includes three data points (filled circles) based on observations made with the polarizing microscope. These points which belong to the mixtures with EO/Na ratios of 3 (X_{PEO} = 0.62), 3.3 (X_{PEO} = 0.64), and 3.7 (X_{PEO} = 0.67), indicate the temperature at the end of the dissolution of the rhombohedral crystals. They complete the phase diagram in the temperature interval between 187 and 309 °C for which no significant thermal event could be detected by DSC.

In Figure 3 it may be seen that below 182 °C the primitive PEO–NaSCN system divides into two subsystems, one being the pseudosubsystem NaSCN–P(EO_3·NaSCN) for which there is no equilibrium and the other being the eutectic subsystem P(EO_3·NaSCN)–PEO. By extrapolating the P(EO_3·NaSCN) liquidus curve (curve a) to the eutectic tie line at 58 °C in the subsystem P(EO_3·NaSCN)–PEO, the composition of the eutectic mixture, $X_{PEO,e}$, can be located at 0.93. This high PEO content of the eutectic mixture explains its small melting point lowering with respect to pure PEO. In Figure 3 it may also be seen that the subsystem P(EO_3·NaSCN)–PEO is apparently not disturbed by the incongruent melting at 182 °C. An explanation for this behavior is that for EO/Na ≥ 3 the incongruent melting of P(EO_3·NaSCN) is delayed because of the absence of solid NaSCN that, if present as

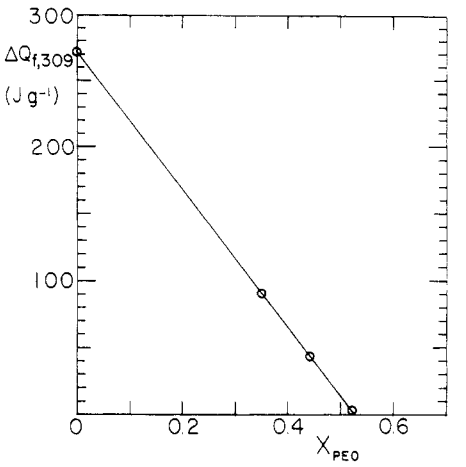

Figure 4. Calorimetric diagram showing the variation of the latent heat per gram of sample, $\Delta Q_{f,309}$, associated with the endotherms recorded at the melting temperature of NaSCN (309 °C) upon the first heating of the PEO–NaSCN mixtures with EO/Na ≤ 2.

in the mixtures with EO/NaSCN < 3, could provide nucleation sites for the salt produced by the disproportionation reaction. This effect results in a metastable extension of the P(EO_3·NaSCN) liquidus curve up to the composition X_{PEO} = 0.62 of the crystalline compound. It makes it possible to define the metastable melting point of this compound at 187 °C, that is at only 5 °C above its incongruent melting point. Above 182 °C, or more rigorously above 187 °C, the PEO–NaSCN system reduces to the solubility curve of NaSCN (curve b), interrupted at 309 °C by a liquid–liquid miscibility gap. The fact that the miscibility gap occurs at the melting temperature of pure NaSCN indicates that one of the two liquid phases in equilibrium with solid NaSCN at this temperature consists of pure NaSCN. On the other hand, the composition of the second liquid phase at 309 °C should be close to X_{PEO} = 0.52 (EO/Na = 2) since, as one can see in Figure 1, the mixture having this composition still exhibits a small endotherm at this temperature in its DSC curve.

A more precise determination of NaSCN solubility at 309 °C can be achieved by a calorimetric analysis of the endotherms observed at this temperature for the mixtures with EO/Na ≤ 2. Such an analysis is shown in Figure 4 where the latent heat corresponding to these endotherms, $\Delta Q_{f,309}$, per gram of sample is plotted as a function of X_{PEO}. As one can see, the data points can be fitted by a straight line having a composition–axis intercept located at X_{PEO} = 0.53. Nevertheless, in spite of the linearity of the data points, this latter result concerning the solubility of NaSCN at 309 °C must be considered with caution because the polymeric liquid phase exhibits some thermal instability at temperatures below the melting point of NaSCN. This could be visually observed under the microscope where upon heating the mixtures at the rate of 5 °C/min the liquid phase became slowly brownish above about 280 °C. In order to examine more quantitatively the consequence of this effect in the conditions of the DSC measurements, the mixture with EO/Na = 2 (X_{PEO} = 0.52) was submitted to various heating cycles between 100 °C and variable upper temperatures in the range from 210 to 320 °C. Each cycle was performed in the DSC apparatus on as-cast specimens. The heating rate was 10 °C/min and the cooling rate was 5 °C/min. After each cycle, the P(EO_3·NaSCN) melting endotherm at 182 °C was recorded upon a second heating and compared to that measured upon the first heating of the as-cast specimen. The results showed that the areas under both endotherms were iden-

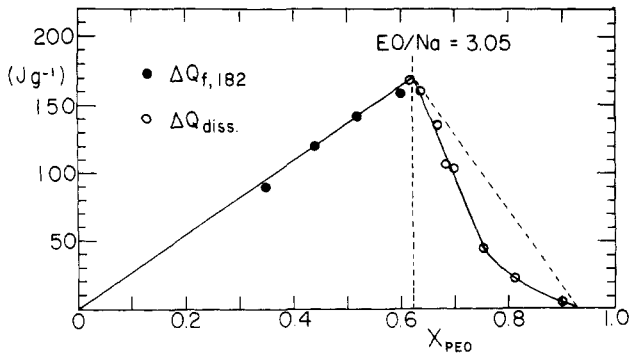

Figure 5. Calorimetric diagram showing the variation of the latent heat, $\Delta Q_{f,182}$, associated with the peritectic endotherms recorded at 182 °C (filled circles) together with the variation of the latent heat, ΔQ_{diss}, associated with the dissolution endotherms of P(EO_3·NaSCN) recorded in the temperature interval between 93 and 187 °C (open circles), both per gram of sample. All data correspond to the first heating of the mixtures.

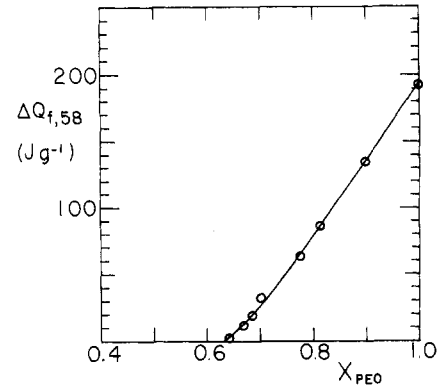

Figure 6. Calorimetric diagram showing the variation of the latent heat per gram of sample, $\Delta Q_{f,58}$, associated with the eutectic endotherms recorded at 58 °C upon the first heating of the PEO–NaSCN mixtures with EO/Na > 3.

tical for all the heating cycles with upper temperatures less than 250 °C. For the cycles with upper temperatures above 250 °C, a decrease in the area of the second endotherm was observed indicating some thermal decomposition. The apparent crystallinity loss for P(EO_3·NaSCN) was 10% for an upper temperature of 270 °C, 22% for 290 °C, and as high as 30% for 320 °C. Therefore, the range of the liquid–liquid miscibility gap depicted in Figure 3 was not determined under well-defined equilibrium conditions. Nevertheless, as will be shown for the PEO–KSCN system whose KSCN component melts at 176 °C, the miscibility gap at the melting point of the pure salt appears to be a genuine feature not resulting from thermal decomposition of the materials.

Calorimetric analysis of the other endotherms in the DSC curves of Figure 1 provides an alternative route to confirm both the 3/1 stoichiometry of the crystalline compound and the composition of the eutectic mixture. Such an analysis is shown in Figure 5 where the latent heat corresponding to the incongruent melting endotherms observed at 182 °C, $\Delta Q_{f,182}$, together with that corresponding to the dissolution endotherms observed in the temperature range 93–187 °C, ΔQ_{diss}, both per gram of sample, are plotted as a function of X_{PEO}. It may be seen that the curves drawn through the $\Delta Q_{f,182}$ and ΔQ_{diss} data points have a point of intersection at X_{PEO} = 0.625 (EO/Na = 3.05) that is very close to the 3/1 stoichiometry. It may also be seen that the $\Delta Q_{f,182}$ data points can be fitted by a straight line that extrapolates to zero at the origin. This behavior is an indication for a complete crystallization of P(EO_3·NaSCN) in the subsystem NaSCN–P(EO_3·NaSCN). On the other hand, the curve drawn through the ΔQ_{diss} data points in the subsystem P(EO_3·NaSCN)–PEO is not linear. It exhibits a pronounced downward curvature that suggests either incomplete crystallization of P(EO_3·NaSCN) or an important exothermic heat of mixing associated with the dissolution process of this compound. Since none of the as-cast mixtures exhibited a glass transition in their DSC curves, it is presumably the nonideality of the dissolution process that accounts for the important curvature in the ΔQ_{diss} plot. This effect will be discussed later in terms of a thermodynamic analysis of the P(EO_3·NaSCN) liquidus curve.

In spite of its pronounced curvature, the ΔQ_{diss} curve in Figure 5 can easily be extrapolated to the composition axis. The intercept, located at X_{PEo} = 0.93, gives the same value for the eutectic composition as that obtained previously by extrapolating the P(EO_3·NaSCN) liquidus curve in the temperature–composition diagram of Figure 3.

Figure 6 shows a plot as a function of X_{PEO} of the latent heat per gram of sample, $\Delta Q_{f,58}$, associated with the eutectic endotherms at 58 °C. The curve drawn through the data points exhibits a small downward curvature together with a composition–axis intercept located at X_{PEO} = 0.63 (EO/Na = 3.13), which is slightly above the composition X_{PEO} = 0.62 of the compound P(EO_3·NaSCN). This indicates that the eutectic crystallization was not quantitative for the mixtures rich in this compound, an effect that can be rationalized by considering that, for these mixtures, the eutectic crystallization has taken place once a large fraction of the material had crystallized under the form of P(EO_3·NaSCN), that is, in the residual liquid surrounding the P(EO_3·NaSCN) crystallites where chain defects were concentrated. Another feature of the curve in Figure 6 is its X_{PEO} = 1 ordinate intercept of 192 J/g that coincides with the latent heat of fusion of the pure PEO sample. This feature appears to be a direct consequence of the high PEO content (X_{PEO} = 0.93) of the eutectic mixture. In turn, it indicates that the eutectic crystallization was nearly quantitative for the mixtures rich in PEO.

In terms of phase equilibria formalism, the disproportionation reaction taking place at 182 °C corresponds to a peritectic equilibrium between two solid phases, solid P(EO_3·NaSCN) and solid NaSCN, and a liquid phase called the peritectic liquid. In the phase diagram of Figure 3 the composition of the peritectic liquid, $X_{PEO,p}$, is given by the point of intersection of the peritectic tie line at 182 °C with the P(EO_3·NaSCN) liquidus curve (curve a). This point is located at X_{PEO} = 0.69 (EO/Na = 4.1), suggesting a tetracoordination of the cation Na^+ in the peritectic liquid. Therefore, on the EO molar unit basis, the peritectic reaction can be written as

$$4(EO_3\text{·NaSCN})_s \rightleftharpoons 3(EO_4\text{·NaSCN})_l + NaSCN_s \quad (1)$$

where the subscripts s and l denote solid and liquid phases, respectively.

Further evidence for a NaSCN solubility governed by the tetracoordination of Na^+ in the liquid state is provided by the observation of a nearly vertical NaSCN liquidus curve (curve b) in the diagram of Figure 3. According to this curve, NaSCN solubility remains close to the ratio EO/Na = 4 over a large temperature interval ranging from 182 °C to about 240 °C. The equilibria leading to this situation can be written as

$$NaSCN_s \underset{}{\overset{K_1(T)}{\rightleftharpoons}} NaSCN_l \quad (2)$$

$$NaSCN_l + 4EO_l \underset{}{\overset{K_2(T)}{\rightleftharpoons}} EO_4{\cdot}NaSCN_l \quad (3)$$

For temperatures below 240 °C it appears that $K_2(T)$ is much greater than $K_1(T)$ thus yielding a global NaSCN content of the liquid phase close to EO/Na = 4 as imposed by reaction 3. For temperatures above 240 °C, and up to the miscibility gap at 309 °C, $K_1(T)$ is no longer negligible and NaSCN solubility increases with temperature. According to the diagram in Figure 3, the relative amount of NaSCN that undergoes dissolution upon heating above 240 °C is rather small. In the best case, that is, for a mixture having EO/Na ratio of 2, it should consist of 0.23 g of NaSCN per gram of sample. This explains why NaSCN dissolution endotherms were scarcely perceptible in the DSC curves of Figure 1. In fact, it is only for the mixtures with EO/Na ratios of 1.45, 2, and 2.8 that one can discern a diffuse base-line anomaly that can be attributed to NaSCN dissolution. For the mixture with EO/Na = 2.8 this anomaly occurs in the temperature interval from 270 to 293 °C while for the mixtures with EO/Na of 1.45 and 2 it extends up to 309 °C and produces an important base-line shift under the melting endotherm of the excess of solid NaSCN.

Thermodynamics of the P(EO_3·NaSCN) Liquidus Curve. The P(EO_3·NaSCN) liquidus curve (curve a) in Figure 3 may be considered as the analogue of the melting point depression curve of P(EO_3·NaSCN) by the diluent PEO. By using the Flory–Huggins concepts, such an approach makes it possible to quantify the interactions between P(EO_3·NaSCN) and PEO by means of the well-known χ parameter.[12] It also provides a route for estimating the heat of mixing of these two polymer species in the liquid state. According to the pronounced downward curvature observed for the P(EO_3·NaSCN) ΔQ_{diss} curve in the calorimetric diagram of Figure 5, an important exothermic heat of mixing is expected for the dissolution process of P(EO_3·NaSCN). This would mainly result from the solvation of P(EO_3·NaSCN) by PEO leading to P(EO_4·NaSCN). Therefore, the χ parameter to be derived from the P(EO_3·NaSCN) liquidus curve should characterize the excess free enthalpy of mixing corresponding to the reaction

$$EO_3{\cdot}NaSCN_l + EO_l \rightleftharpoons EO_4{\cdot}NaSCN_l \quad (4)$$

As shown by Nishi and Wang,[12] the melting point depression of a crystalline polymer (polymer 2) by a polymeric diluent (polymer 1) should be essentially governed by the magnitude of the Flory–Huggins χ parameter according to the relation

$$\frac{1}{T_m} - \frac{1}{T^0_m} = -\frac{RV_{2,u}}{\Delta H_{2,u} V_{1,u}} \chi \varphi_1^2 \quad (5)$$

where $\Delta H_{2,u}$ is the enthalpy of fusion per mole of repeating unit of polymer 2, $V_{2,u}$ and $V_{1,u}$ are the molar volumes of the repeating units of polymer 2 and 1, respectively, φ_1 is the volume fraction of the polymeric diluent, and R is the perfect gas constant.

By both assuming that the entropy of mixing of the two polymers is negligible and that χ is composition independent, one can relate this latter parameter to the enthalpy of mixing, ΔH_m^v, per volume unit of mixture.[13]

$$\Delta H_m^v = B\varphi_1\varphi_2 \quad (6)$$

with

$$B = \frac{RT}{V_{1,u}} \chi \quad (7)$$

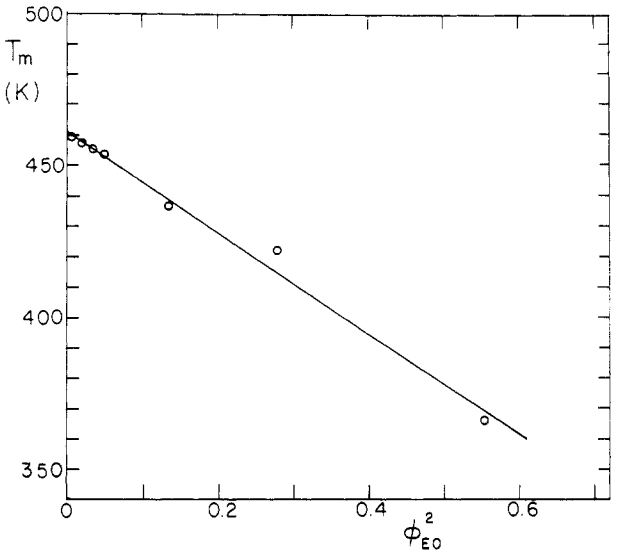

Figure 7. Plot according to eq 8 of the peak temperature, T_m, of the P(EO_3·NaSCN) dissolution endotherms as a function of the square of the volume fraction, φ_{EO}, of PEO in excess of the stoichiometric composition.

Parameter B represents the interaction energy density for the unlike polymer pair.[14] In the case of a negligible entropy of mixing, B should be temperature independent. With this latter assumption eq 5 can be rearranged to yield

$$T_m = T^0_m + \frac{BV_{2,u}T^0_m}{\Delta H_{2,u}} \varphi_1^2 \quad (8)$$

Figure 7 shows a plot of T_m as a function of φ_{EO}^2 based on the peak position of the dissolution endotherms of P(EO_3·NaSCN). The quantity φ_{EO} corresponds to the volume fraction of the EO units in excess of the 3/1 stoichiometry. It has been calculated by assuming that the density ratio $\rho_{P(EO_3{\cdot}NaSCN)}/\rho_{PEO}$ is temperature independent and close to that measured at 25 °C for the crystalline materials. Density measurements carried out at 25 °C by the flotation method in chloroform–heptane mixtures yielded the quantities $\rho_{P(EO_3{\cdot}NaSCN)}$ = 1.33 g/cm^3 and ρ_{PEO} = 1.23 g/cm^3 for the crystalline materials.

The data points in Figure 7 can be fitted by a straight line having a temperature-axis intercept of 461 ± 2 K (T^0_m = 188 ± 2 °C) and a slope of −165 ± 8 K that yields a B value of −82 ± 4 J/cm^3 which in turn yields a χ value of −1.18 ± 0.06 at 25 °C. The latter two quantities have been calculated by using the value of 172 J/g determined by DSC for the heat of fusion of P(EO_3·NaSCN), and the quantities $V_{EO_3{\cdot}NaSCN}$ = 160 cm^3/mol and V_{EO} = 35.8 cm^3/mol estimated from the densities of the corresponding solids at 25 °C.

The large magnitude of the χ parameter is a clear indication that a chemical reaction of the type described by eq 4 takes place in the dissolution process of P(EO_3·NaSCN). In that respect, an analogy can be made with the PEO–glutaric acid eutectic system previously studied by Gryte et al.[15] that involves hydrogen bonding between the two components in the liquid state. For this system, the B value determined from the melting point depression of PEO is −28 ± 5 J/cm^3 yielding a χ value of −1.3 ± 0.2 at 25 °C. The similarity between the χ values of the two systems indicates that the excess free enthalpy change associated with the solvation of P(EO_3·NaSCN) by PEO is of the same order of magnitude as that for the solvation of PEO by glutaric acid, the latter being a dicarboxylic acid capable of forming two hydrogen bonds per EO unit.

Contrary to the PEO–NaSCN system, the PEO–glutaric system does not form a crystalline compound. In fact, strong interaction between the components of a binary mixture is not the unique condition for the formation of a crystalline compound, particularly if one of the components is a polymer. A more important condition is the existence of a crystal structure for this compound that has a lower free enthalpy than the melt. For a polymer–small molecule compound such a structure should consist of a packing of parallel chains having either a zigzag or helical conformation that can accommodate the small molecule adducts. It is presumably for that reason that the PEO–NaSCN system crystallizes in the form of the compound $P(EO_3{\cdot}NaSCN)$ instead of $P(EO_4{\cdot}NaSCN)$, though the latter compound is apparently more stable than the former in the liquid state.

Inserting into eq 6 the quantity $B = -82$ J/cm^3 obtained in the foregoing analysis of the $P(EO_3{\cdot}NaSCN)$ liquidus curve, one can predict a maximum value of -21 J/cm^3 for the heat of mixing of $P(EO_3{\cdot}NaSCN)$ with PEO. This value, which corresponds to the case where $\varphi_1 = \varphi_2$ in eq 6, is clearly insufficient to account for the pronounced curvature of the ΔQ_{diss} plot in Figure 5. Only a B value about 3 times as large as the present value would give an acceptable fit to the experimental data. Partial crystallization of $P(EO_3{\cdot}NaSCN)$ might also account for the ΔQ_{diss} depression. However, as it will be shown in the next sections, this would have led to a supercooled amorphous phase departing from the eutectic composition and thereby unable to give rise to eutectic crystallization. Another explanation for the above discrepancy might be that the B value is correct but that the assumption made in eq 6 that the entropy of mixing is negligible does not hold for the present case. If such is the situation, ΔH_m^v in eq 6 should be replaced by $\Delta G_m^v = \Delta H_m^v - T\Delta S_m^v$ where ΔG_m^v and ΔS_m^v are the excess free enthalpy and the excess entropy associated with the solvation reaction of $P(EO_3{\cdot}NaSCN)$ by PEO. In fact, a negative entropy change for this process would result in a larger exothermic value of ΔH_m^v, in better agreement with the experimental data.

Melt-Crystallized Mixtures. In order to examine the reversibility of the peritectic reaction, the foregoing mixtures have been recrystallized from the melt by a slow cooling to 0 °C at 5 °C/min after a complete melting of their macromolecular phase at 210 °C for a period of 15 min. Except for the mixture with EO/Na = 8, the DSC curves recorded upon this cooling all exhibited one or two exothermic peaks that can be attributed to crystallization phenomena. The mixtures having EO/Na ratios ranging from 1 to 4, that is those having a PEO content equal or lesser than that of the peritectic liquid, all exhibited an invariant exothermic peak at 147 °C that can be attributed to the crystallization of the $P(EO_3{\cdot}NaSCN)$ compound. Among these mixtures, those with EO/Na > 3 also exhibited a second invariant exothermic peak at 23 °C that can be attributed to the crystallization of the eutectic liquid. Therefore, with respect to their respective melting points at 182 and 58 °C, both the solid compound and the eutectic mixture crystallize with a supercooling of 35 °C. On the other hand, at the same cooling rate of 5 °C/min, the crystallization peak of the pure PEO sample occurred at 42 °C with a less important supercooling of 20 °C. In any case, the supercooling was hardly affected by a diminution of the cooling rate. For instance, at a cooling rate of 0.625 °C/min, the two crystallization peaks of the mixture with EO/Na = 4 underwent a shift of only 3 °C toward higher temperatures, indicating that the supercooling effect was principally due to molecular nucleation.

Concerning the mixtures having EO/Na ratios greater than 4, only those with EO/Na ratios of 4.3 and 5.6 exhibited a $P(EO_3{\cdot}NaSCN)$ crystallization peak prior to their eutectic crystallization at 23 °C. These peaks occurred at 145 and 125 °C, respectively, that is with a supercooling of 35 °C with respect to the $P(EO_3{\cdot}NaSCN)$ liquidus curve depicted in the phase diagram of Figure 3. On the other hand, the mixture with EO/Na = 8 did not exhibit any crystallization peak, while the mixture with EO/Na = 16 only exhibited a eutectic crystallization peak at 23 °C. Nevertheless, as will be shown shortly, these latter two PEO-rich mixtures could recover their initial crystallinity upon an isothermal annealing of 4 h at 35 °C.

The slower crystallization rate of $P(EO_3{\cdot}NaSCN)$ observed for the mixtures with EO/Na ratios of 8 and 16 is the result of two distinct effects associated with the lower NaSCN content of these mixtures. One of these effects is the need, with decreasing NaSCN content, for a more extensive transport of NaSCN through the supercooled melt in the $P(EO_3{\cdot}NaSCN)$ formation process. The other effect is the greater viscosity of the melt at the lower $P(EO_3{\cdot}NaSCN)$ crystallization temperatures expected for the mixtures poor in NaSCN. Since the rate of diffusion of NaSCN is governed by the viscosity of the melt, the net result of both these effects is a substantial decrease in the rate of formation of $P(EO_3{\cdot}NaSCN)$. On the other hand, for straightforward reasons, the eutectic crystallization cannot occur for supercooled melts whose composition departs from the eutectic composition. This explains why the eutectic crystallization was not observed for the mixture with EO/Na = 8 ($X_{PEO} = 0.75$) but occurred for the mixture with EO/Na = 16 ($X_{PEO} = 0.90$), the latter being close to the eutectic composition ($X_{PEO,e} = 0.93$). In turn, the occurrence at 23 °C of the eutectic crystallization for the mixtures with $3 < EO/Na \leq 5.6$ is an indication that their residual melts at this temperature had a composition close to the eutectic composition.

The foregoing mixtures cooled at 5 °C/min were submitted to an annealing of 4 h at 35 °C after which DSC heating curves were recorded again at a rate of 10 °C/min. Upon annealing all the mixtures recovered their initial amount of eutectic solid, as could be judged by the intensity of their eutectic endotherms. Nevertheless, the eutectic melting endotherms of these mixtures exhibited a lowering of 4 °C with respect to those recorded for the as-cast mixtures. Since an identical lowering of 4 °C was also observed for the melting endotherm of the pure PEO sample recrystallized under the same conditions, it appears that PEO chain folding was responsible for this change of behavior. Indeed, as reported by Buckley and Kovacs,[16] bulk crystallization of a PEO sample having the same molecular weight ($\bar{M}_n = 4 \times 10^3$) as the present sample can yield crystallites consisting of either once folded or fully extended PEO chains (or both), depending upon the crystallization temperature. According to their findings, isothermal crystallizations carried out below 47 °C yield a large fraction of once folded chain crystallites that melt 4 °C below the melting point of extended chain crystallites which appear to be thermodynamically more stable above 47 °C. They also showed that PEO chain unfolding could occur during the heating of the once folded chain crystallites, but only for heating rates slower than about 8 °C/min. Therefore, the 4 °C difference observed for the eutectic invariant indicates that the PEO crystallites in the recrystallized mixtures consisted of once folded chains while those in the as-cast mixtures consisted of fully extended chains. Indeed, this was confirmed by submitting some of the recrystallized specimens to an annealing of half

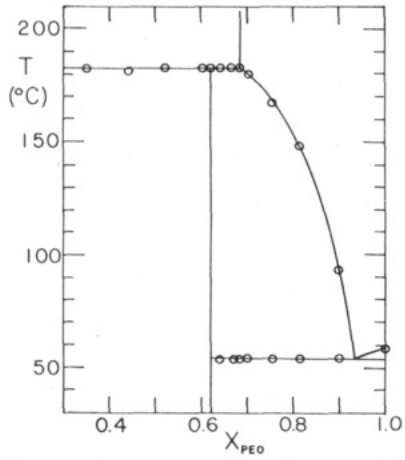

Figure 8. Temperature–composition diagram similar to that of Figure 3 showing the disappearance of the metastable segment of the P(EO_3·NaSCN) liquidus curve after melt recrystallization of the mixtures. The other difference is a eutectic tie line at 54 °C instead of 58 °C. Melt recrystallization was carried out by a slow cooling from 210 to 0 °C at a rate of 5 °C/min followed by an annealing of 4 h at 35 °C.

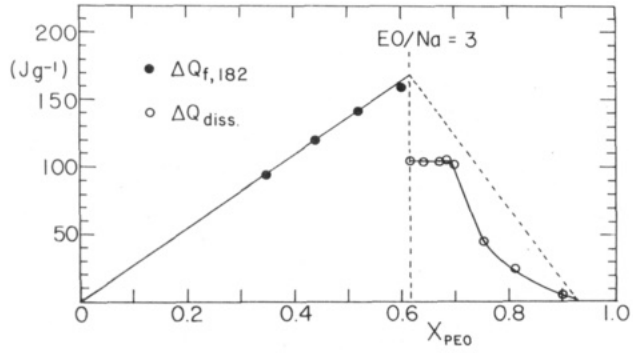

Figure 9. Calorimetric diagram similar to that of Figure 5 showing the incompleteness of the reverse path of the peritectic reaction during melt recrystallization of the mixtures in the composition interval from X_{PEO} = 0.62 (EO/Na = 3) to X_{PEO} = 0.685 (EO/Na = 4). The conditions used for the melt recrystallization are described in the legend of Figure 8.

an hour at 51 °C in the DSC apparatus. Upon a subsequent heating, the annealed specimens exhibited two distinct eutectic endotherms at 54 and 58 °C, respectively, indicating that some PEO chain unfolding occurred during the annealing at 51 °C.

The peak temperatures of the thermal events observed in the DSC curves of the recrystallized mixtures are summarized in Figure 8 under the form of a second temperature–composition diagram. In addition to the 4 °C change concerning the eutectic invariant, this diagram also shows a significative difference concerning the peritectic invariant at 182 °C. It may be seen that this invariant now persists up to the composition of the peritectic liquid (EO/Na = 4). In other words, contrary to the as-cast mixtures, the recrystallized mixtures do not exhibit a metastable congruent behavior in the composition interval from EO/Na = 3 to EO/Na = 4. This indicates that some solid NaSCN remained present in these mixtures at the end of their melt recrystallization and provided nucleation sites for the subsequent P(EO_3·NaSCN) disproportionation reaction at 182 °C. This calls for a more quantitative examination of the peritectic reaction reversibility by means of the calorimetric data. For that purpose, Figure 9 shows a plot of the latent heat per gram of sample associated with the peritectic reaction, $\Delta Q_{f,182}$, as a function of X_{PEO}. Also plotted in the same diagram are the ΔQ_{diss} data points associated with the P(EO_3·NaSCN) dissolution peaks recorded for the complementary mixtures with EO/Na > 4. It may be seen that all the data points in Figure 9, except those for the mixtures in the composition interval from X_{PEO} = 0.62 (EO/Na = 3) to X_{PEO} = 0.685 (EO/Na = 4), are nearly superimposable on the data points depicted in Figure 5 for the as-cast mixtures. It may also be seen that $\Delta Q_{f,182}$ decreases abruptly from 172 to 105 J/g at EO/Na = 3 and remains nearly unchanged up to EO/Na = 4. This indicates that the reaction between solid NaSCN and the peritectic liquid, that is, the reverse reaction in eq 1, was not quantitative during the cooling at 5 °C/min.

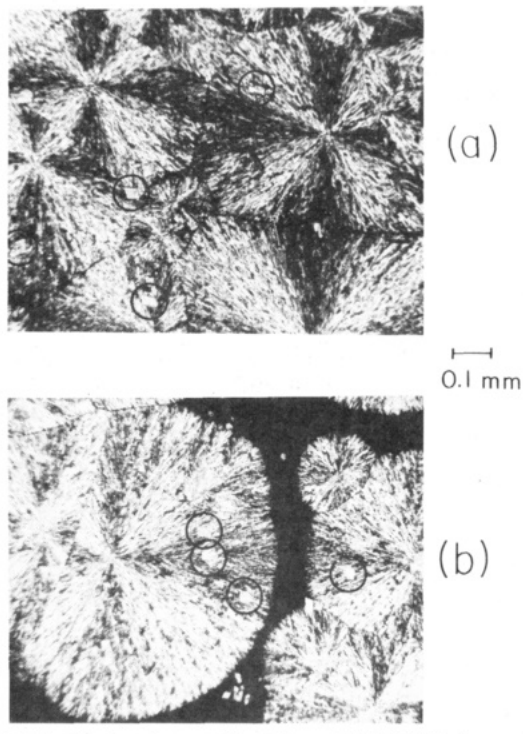

Figure 10. Photomicrographs taken at 100 °C during melt recrystallization of the PEO–NaSCN mixtures with EO/Na = 2 (a) and EO/Na = 3.7 (b) showing some NaSCN rhombohedral crystals (encircled in the photographs) frozen within P(EO_3·NaSCN) spherulites.

From Figure 10 which shows micrographs taken at 100 °C during the melt recrystallization of the mixtures with EO/Na ratios of 2 and 3.7, it may be seen that in both cases some of the large NaSCN rhombohedral crystals formed upon the first melting of these mixtures remained frozen within the P(EO_3·NaSCN) spherulites crystallized from the melt. This indicates that once the large NaSCN crystals were surrounded by solid P(EO_3·NaSCN) during the melt crystallization process they no longer could participate to the reverse path of the peritectic reaction. Such a behavior is not a particularity of the present system. It is frequently encountered in the case of small molecule systems giving rise to a peritectic reaction.[17] According to the calorimetric diagram in Figure 9, this effect severely perturbed the reversibility of the peritectic reaction in the case of the mixtures with EO/Na ≥ 3 in which the NaSCN solid phase consisted of large rhombohedral crystals only, but not in the case of the mixtures with EO/Na < 3 which contained granular clusters of much smaller NaSCN crystals in addition to the large rhombohedral crystals. Therefore, it is because of the greater specific surface of the NaSCN solid phase present in the latter mixtures that their peritectic reaction was quantitatively reversible upon slow cooling at 5 °C/min.

Quenched Mixtures. In view of the slow crystallization rate observed for the P(EO_3·NaSCN) compound in the case

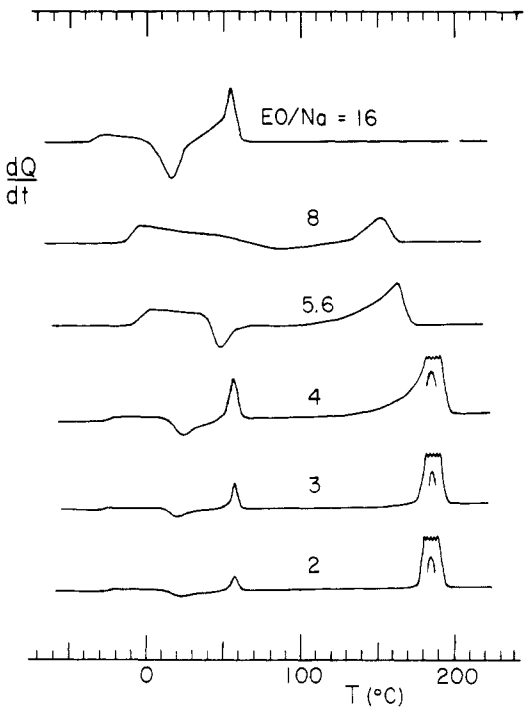

Figure 11. DSC heating curves recorded at 40 °C/min for PEO–NaSCN mixtures quenched after a melting period of 15 min at 210 °C. The quenching, from 210 to −100 °C, was carried out in the DSC apparatus at a cooling rate of 320 °C/min.

of the mixture with EO/Na = 8, it was interesting to examine the crystallinity of some of the PEO–NaSCN mixtures after a rapid cooling from 210 to −100 °C. Such a cooling was carried out in the DSC apparatus at a rate of 320 °C/min, after which a heating curve was recorded at the rate of 40 °C/min. This greater heating rate was chosen in order to increase the sensitivity of the DSC method for a better detection of the glass transition anomalies. In fact, as shown in Figure 11, all the mixtures submitted to the rapid cooling exhibit a glass transition at a temperature located in the interval between −36 and −8 °C. They also exhibit a crystallization exotherm followed by either one or two fusion endotherms at higher temperatures. On the basis of the relative intensities of the exothermic and endothermic events, it may be concluded that the quenched mixtures with PEO contents greater than the peritectic composition (EO/Na > 4) were almost completely amorphous while those with PEO contents equal or lesser than the peritectic composition (EO/Na ⩽ 4) were highly crystalline.

Figure 12 shows a plot of the T_g's observed in Figure 11 as a function of X_{PEO}. It may be seen that a discontinuity occurs in this plot at the composition of the peritectic liquid (EO/Na = 4). Below this composition, T_g remains invariant at about −28 °C. Above it, T_g increases abruptly toward a maximum value of −8 °C at X_{PEO} = 0.75 (EO/Na = 5.6) and then decreases substantially with further increase of X_{PEO}. It may also be seen that the curve drawn through these latter data points extrapolates to −69 °C at X_{PEO} = 1, a result in good agreement with the T_g(PEO) value of −73 °C obtained by Robeson et al.[18] from a similar extrapolation procedure applied to the T_g's of amorphous miscible blends of PEO ($\bar{M}_w = 4 \times 10^6$) with a phenoxy resin. Note that quenching of pure PEO of either low or high molecular weight does not yield an amorphous material.

Inspection of Figure 11 shows that all the mixtures with EO/Na ratios equal or lesser than 4, including the mixture with EO/Na = 2, exhibit a crystallization exotherm at

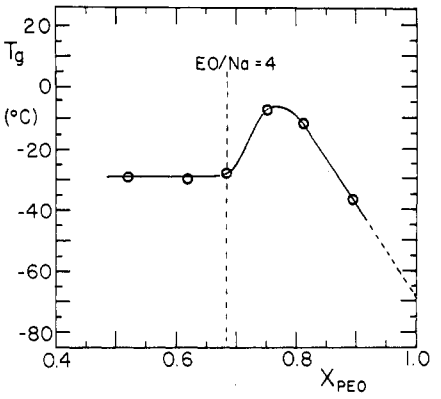

Figure 12. Plot of the glass transition temperature, T_g, of the PEO–NaSCN quenched mixtures as a function of their PEO weight fraction, X_{PEO}.

20–23 °C followed by a melting endotherm at 59 °C that both can be attributed to the presence of a supercooled phase having the composition of the eutectic mixture. This indicates that under rapid cooling the reverse path of the peritectic reaction was no longer quantitative for the mixtures with EO/Na < 3. On the other hand, among the complementary mixtures with EO/Na ratios greater than 4, only the mixture with EO/Na = 16 exhibits a crystallization exotherm upon heating that is close to the eutectic crystallization exotherms observed for the preceding mixtures. The other two mixtures (EO/Na = 5.6 and 8) each exhibits a crystallization exotherm at much higher temperatures, indicating that their amorphous phase was substantially richer in NaSCN than the eutectic mixture. The mixture with EO/Na = 8 exhibits a very broad crystallization exotherm centered at 90 °C that suggests a crystallization path following the P(EO_3·NaSCN) liquidus curve in Figure 3. As for the EO/Na = 16 mixture, the EO/Na = 8 mixture was completely amorphous after quenching. Apparently, this was not the case for the mixture with EO/Na = 5.6 which exhibits a sharp crystallization exotherm at 50 °C, that is in between those of the mixtures with EO/Na ratios of 8 and 16, indicating that the composition of the amorphous phase in this latter mixture was closer to the eutectic composition than that of the completely amorphous EO/Na = 8 mixture.

A last remark concerns the T_g values of the semicrystalline mixtures. The invariant T_g at −28 °C attributed to the supercooled eutectic phase in the mixtures with EO/Na < 4 is definitely higher than the T_g value of −48 °C one can estimate for a supercooled eutectic mixture by extrapolating the T_g curve in Figure 12 to the eutectic composition ($X_{PEO,e}$ = 0.93). Similarly, the T_g value of −8 °C for the mixture with EO/Na = 5.6 is higher than that below −13 °C expected for a completely amorphous mixture having an EO/Na ratio greater than 8 as it is the case for the amorphous phase in the EO/Na = 5.6 mixture. The observation of higher T_g values for the amorphous phase in the semicrystalline mixtures is a consequence of the dispersion of this phase at the interface of the P(EO_3·NaSCN) crystallites, that is in regions where chain mobility is restricted by either tie points or entanglements.

PEO–KSCN System. Figure 13 shows a temperature–composition diagram depicting the peak positions of the endothermic events recorded at a heating rate of 10 °C/min for a series of as-cast PEO–KSCN mixtures having EO/K molar ratios ranging from 0.5 to 15. The main features of this diagram are two invariant equilibria located at 95 and 176 °C, respectively. The transition at 176 °C coincides with the melting point of pure KSCN. It is observed for all the mixtures having EO/K ⩽ 4 (X_{PEO} ⩽

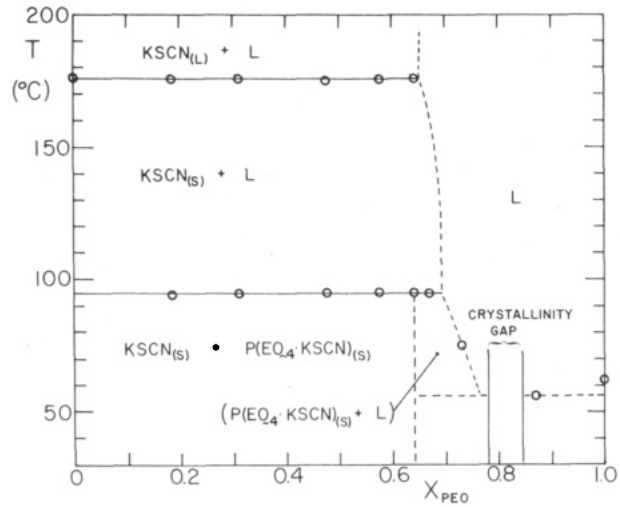

Figure 13. Temperature–composition diagram of the PEO–KSCN system depicting the peak positions of the fusion and dissolution endotherms recorded at 10 °C/min upon the first heating of the mixtures. Not included in this diagram is an additional tie line at 140 °C that corresponds to a crystalline transition for KSCN. This latter transition was observed for all the mixtures that gave rise to a transition at the melting temperature of KSCN (176 °C).

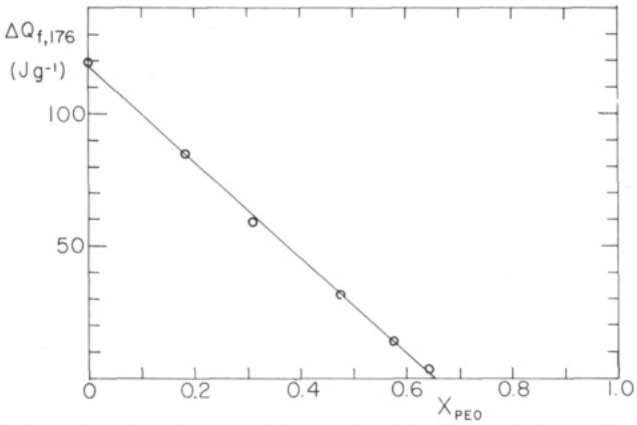

Figure 14. Calorimetric diagram showing the variation of the latent heat per gram of sample, $\Delta Q_{f,176}$, associated with the endotherms recorded at the melting temperature of KSCN (176 °C) upon the first heating of the PEO–KSCN mixtures with EO/K $\leq$ 4.

0.64). Associated with this transition was a third but less intense invariant endotherm located at 140 °C (not shown in Figure 13) that corresponds to a crystalline transition occurring in the pure salt.[19,20] Therefore, as for the PEO–NaSCN system, the present system exhibits a liquid–liquid miscibility gap at the melting point of the pure salt. Figure 14 shows a calorimetric diagram in which the latent heat per gram of sample, $\Delta Q_{f,176}$, corresponding to the endotherm at 176 °C is plotted as a function of X_{PEO}. The curve drawn through the $\Delta Q_{f,176}$ data points has a composition–axis intercept located at X_{PEO} = 0.65 (EO/K = 4.1), indicating that KSCN solubility in liquid PEO is close to 35% by weight at the melting point of KSCN. Also, as for the PEO–NaSCN system, the other invariant transition observed at 95 °C corresponds to an incongruent melting of a crystalline compound of the type P(EO$_x$·KSCN) that decomposes to yield solid KSCN and a peritectic liquid.

Figure 15 shows micrographs taken at 105 °C for mixtures with EO/K ratios of 2, 4, and 4.5 in which the KSCN crystals that have grown in the peritectic liquid appear under the form of dendrites of various shapes. In the case of the mixtures with EO/K ratios of 2 and 4 the dendrites

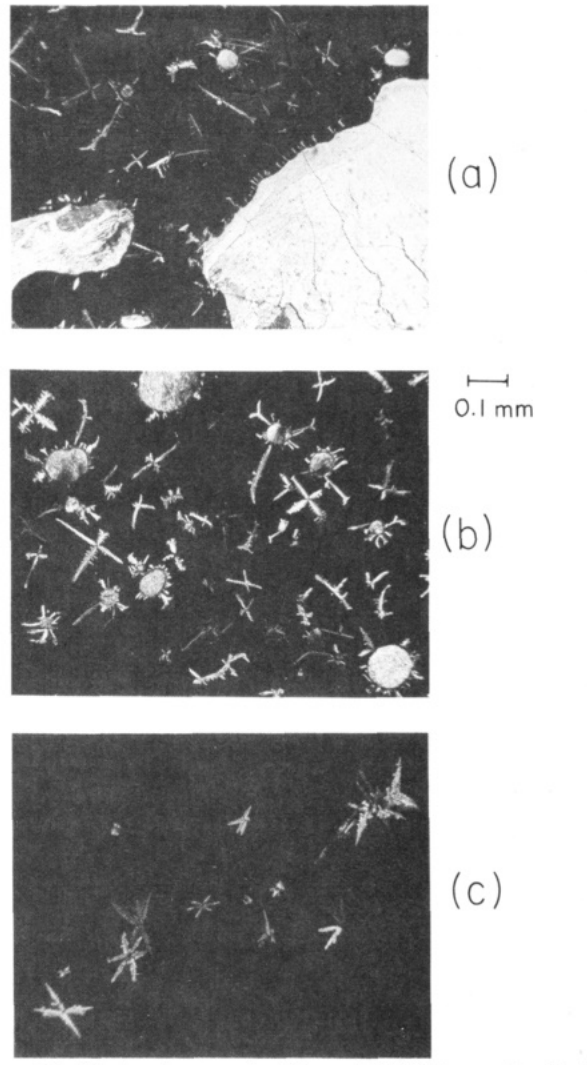

Figure 15. Photomicrographs taken at 105 °C upon the first heating of PEO–KSCN mixtures with EO/K = 2 (a), EO/K = 4 (b), and EO/K = 4.5 (c), respectively. The dark areas correspond to the peritectic liquid.

are seen together with some granular domains of solid KSCN that were already present in the mixtures prior to their incongruent melting. These domains are absent in the case of the mixture with EO/K = 4.5, indicating that the stoichiometry of the P(EO$_x$·KSCN) crystalline compound lies somewhere between x = 4 and x = 4.5.

The other particularities of the as-cast PEO–KSCN system are a crystallinity gap in the composition interval between X_{PEO} = 0.78 (EO/K = 8) and X_{PEO} = 0.84 (EO/K = 12) and a partial crystallinity for all the other mixtures with EO/K $\geq$ 4.5 as indicated by a sharp glass transition anomaly in their DSC curves. Among these latter mixtures, only that with EO/K ratio of 15 exhibited an endothermic peak lying at a temperature (56 °C) below the melting point (62 °C) of the pure PEO sample. On the other hand, because of the semicrystalline character of the mixtures with EO/K ratios of 4.5 and 6 it was illusory to get the correct stoichiometry of the compound P(EO$_x$·KSCN) by means of a calorimetric diagram based on the intensity of the thermal events associated with either the fusion or the dissolution of this compound. As shown in Figure 16, such a diagram consists of two linear segments that intersect at X_{PEO} = 0.64 (EO/K = 4), albeit the mixture having this composition is definitively substoichiometric in PEO on the basis of the preceding observations made under the microscope.

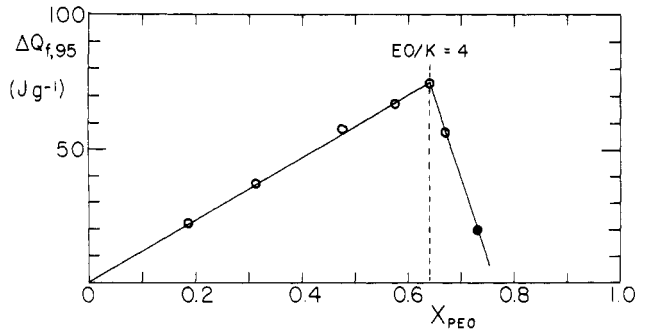

Figure 16. Calorimetric diagram showing the variation of the latent heat per gram of sample, $\Delta Q_{f,95}$, associated with the peritectic endotherms recorded at 95 °C upon the first heating of the PEO–KSCN mixtures. Also included is a data point (filled circle) corresponding to the dissolution endotherm recorded at 75 °C for the mixture with EO/K = 6 (X_{PEO} = 0.73).

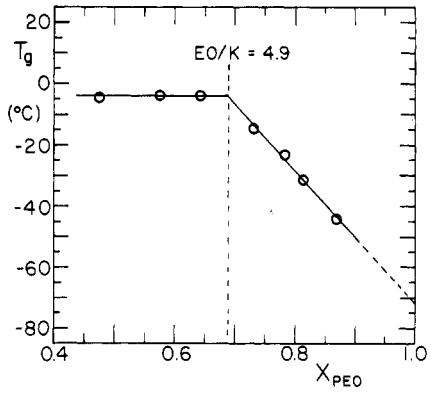

Figure 17. Plot of the glass transition temperature, T_g, of the PEO–KSCN quenched mixtures as a function of their PEO weight fraction, X_{PEO}.

In contrast to the PEO–NaSCN mixtures, once melted at a temperature above the melting point of the crystalline compound, all the PEO–KSCN mixtures investigated in the present work could be quenched under the form of completely amorphous polymeric phases either saturated or not saturated by KSCN. Moreover, a cooling rate of 40 °C/min was sufficiently rapid for obtaining the completely amorphous polymeric phase characteristic of these mixtures. The variation of their T_g as a function of X_{PEO} is shown in Figure 17. The T_g measurements were carried out at a heating rate of 40 °C/min after a quenching from 120 to −100 °C, also performed at 40 °C/min. Since the T_g data in Figure 17 are not perturbed by the presence of polymeric crystallinity, their composition dependence is much more straightforward than that depicted in Figure 12 for the PEO–NaSCN quenched mixtures. With increasing X_{PEO}, T_g first remains invariant at −4 °C up to X_{PEO} = 0.69 (EO/K = 4.9) and then decreases linearly with X_{PEO} to extrapolate to a T_g(PEO) value of −72 °C at X_{PEO} = 1. Note that this latter value is close to the foregoing T_g(PEO) value of −69 °C obtained by extrapolating the T_g data of the PEO–NaSCN quenched mixtures depicted in Figure 12.

Among the PEO–KSCN quenched mixtures, only that with EO/K = 15 exhibited a crystallization exotherm upon heating at 40 °C/min. This exotherm occurred at 21 °C and was followed by an endotherm of about the same intensity located at 53 °C. In fact, the behavior of this mixture was very similar to that of the mixture with EO/Na = 16 shown in Figure 11, except for its extent of crystallization upon heating which was about 5 times less than that of the sodium-containing mixture. This latter feature together with the absence of a crystallization exotherm for the other PEO–KSCN mixtures can be explained by a slower diffusion rate of KSCN with respect to NaSCN resulting from the larger size of the potassium ion.

From the invariance of T_g at −4 °C up to X_{PEO} = 0.69 in the plot of Figure 17, it may be concluded that this latter composition characterizes KSCN solubility in amorphous PEO at −4 °C. Therefore, over the large temperature interval between −4 and 176 °C, KSCN solubility in liquid PEO only increases from 31% to 35% by weight, a behavior that is indicative of complex formation taking place in the liquid phase in equilibrium with either the solid compound or the solid salt above the melting temperature of the solid compound. The apparent coordination number of this complex in the liquid state appears to be close to 5 (X_{PEO} = 0.69), which is slightly greater than that close to 4 observed for NaSCN. Here again, this difference might be explained by the larger size of the potassium ion.

Finally, by comparing the T_g data in Figure 17 with those of the PEO–NaSCN mixtures in Figure 1, it may be concluded that PEO chain mobility is less affected by the presence of KSCN than by that of NaSCN. For instance, at the composition X_{PEO} = 0.82 for which both systems were completely amorphous after quenching, a T_g lowering of 19 °C is observed for PEO–KSCN (EO/K = 10) with respect to PEO–NaSCN (EO/Na = 8). This difference is presumably due to the weaker energy of the individual ion–dipole interactions in the case of the potassium ion. In other words, the cross-linking effect produced by these interactions is less effective for the PEO–KSCN system due to the smaller charge density of the potassium ion.

Conclusion

The present thermal study performed on PEO–NaSCN and PEO–KSCN mixtures of various compositions reveals great similarities between the two systems. Their common characteristics are first the formation of a single crystalline compound that melts incongruently to yield the solid salt and a peritectic liquid and second a liquid–liquid miscibility gap occurring at the melting point of the pure salt. The PEO content of the compound with NaSCN is close to 62 ± 1% by weight and its melting point is 182 °C. This composition corresponds to the formula P(EO_3·NaSCN) previously found by Hibma.[9] The composition of the compound with KSCN could not be determined with the same accuracy. Its PEO content lies between 64% and 67% by weight and its melting point is 95 °C. This yields the formula P(EO_x·KSCN) with x lying between 4 and 4.5. For this latter compound, Hibma[9] proposed a x = 4 stoichiometry based on a x = 4.2 experimental value obtained from the weight increase of a PEO film after its dipping in an ethyl acetate KSCN solution.

Taking advantage of the high crystallinity of the PEO–NaSCN mixtures over the whole composition range, it has been possible to construct a complete phase diagram for this system. Because of the peritectic reaction, the P(EO_3·NaSCN) compound cannot participate to a eutectic equilibrium with the solid salt. In turn, it forms a eutectic mixture with solid PEO whose PEO content is close to 93% by weight. The corresponding eutectic tie line in the phase diagram is located at about 4 °C below the melting point of pure PEO. Contrary to the PEO–NaSCN system, the PEO–KSCN system exhibits either partial crystallinity or absence of crystallinity in the PEO-rich region above the composition of the solid compound. For that reason, it has not been possible to determine whether this compound forms a eutectic mixture with PEO. Among the mixtures studied in this region, only that with the largest PEO content (87% by weight) exhibited a melting temperature below that of pure PEO The corresponding

melting point depression of 6 °C suggests the possibility for a eutectic mixture having about the same composition as that of the PEO–NaSCN system.

Either system exhibits a nearly vertical salt liquidus curve above the melting point of the solid compound. This reveals that complex formation also takes place in the liquid phase in equilibrium with the solid salt. The apparent coordination number of this complex has been estimated to be close to 4 for NaSCN and close to 5 for KSCN. In the case of the PEO–NaSCN system, it has been possible to rationalize two distinct features related to the liquidus curve of the solid compound in terms of a complex formation in the liquid phase. One of these features is the large χ value of −1.2 derived from the thermodynamic analysis of the P(EO_3·NaSCN) liquidus curve by means of Flory–Huggins concepts. The other is the important downward curvature observed in the variation of the latent heat of dissolution of the solid compound as a function of the composition in the subsystem P(EO_3·NaSCN)–PEO. Both can be explained by an important exothermic interaction resulting from the solvation of the 3/1 compound by PEO yielding a 4/1 complex in the liquid phase.

As a result of the peritectic reaction that occurs for both systems, bulk recrystallization of the solid compound in mixtures having a salt content greater than that of the peritectic liquid is not a simple liquid–solid phase transition process. Indeed, prior to their solid compound crystallization, all these mixtures, including the stoichiometric mixture, are characterized by the presence of the solid salt dispersed in a liquid phase substoichiometric in salt. This leads to a peculiar situation in which the dissolution rate of the salt, as well as its diffusion rate in the liquid phase, can contribute to a reduction of the rate of crystallization of the solid compound. In this domain of composition, it has been observed that a moderate cooling rate of 40 °C/min is sufficiently rapid for inhibiting the crystallization of the compound with KSCN, while the compound with NaSCN crystallizes readily even at the much greater cooling rate of 320 °C/min. This indicates that diffusion rate of KSCN is considerably smaller than that of NaSCN, a feature that can be explained by the larger size of the potassium ion but also by the greater coordination number of its solvate in the liquid phase. On the other hand, it has been observed that because of the prompt crystallization of the compound with NaSCN, the large NaSCN crystals formed during the first melting of the mixtures are encapsulated by the crystallizing compound and do not participate in the reverse path of the peritectic reaction. Therefore, it appears that contrary to solvent crystallization, bulk crystallization of the stoichiometric mixtures of both systems cannot yield the pure crystalline compounds.

Acknowledgment. This work was supported by Natural Sciences and Engineering Research Council of Canada and the Quebec Ministry of Education.

References and Notes

(1) Blumberg, A. A.; Wyatt, J. *J. Polym. Sci., Polym. Lett. Ed.* **1966**, *4*, 653.
(2) Iwamoyo, R.; Saito, Y.; Ishihara, H.; Tadokoro, H. *J. Polym. Sci., Polym. Phys. Ed.* **1968**, *6*, 1509.
(3) Wright, P. V. *Br. Polym. J.* **1975**, *7*, 319.
(4) Armand, M. B.; Chabagno, J. M.; Duclot, M. J. In *Fast Ion Transport in Solids*; Vashishta, P., Mundy, J. N., Shenoy, G. K., Eds.; Elsevier North Holland: New York, 1979; p 131.
(5) Weston, J. E.; Steele, B. C. H. *Solid State Ionics* **1981**, *2*, 347.
(6) Papke, B. L.; Dupon, R.; Ratner, M. A.; Shriver, D. F. *Solid State Ionics* **1981**, *5*, 685.
(7) Berthier, C.; Gorecki, W.; Minier, M.; Armand, M. B.; Chabagno, J. M.; Rigaud, P. *Solid State Ionics* **1983**, *11*, 91.
(8) Minier, M.; Berthier, C.; Gorecki, W. *J. Chim. Phys.* **1984**, *45*, 739.
(9) Hibma, T. *Solid State Ionics* **1983**, *9–10*, 1101.
(10) Robitaille, C.; Fauteux, D. *J. Electrochem. Soc.* **1986**, *133*, 315.
(11) Lee, Y. L.; Crist, B. *J. Appl. Phys.* **1986**, *60*, 2683.
(12) Nishi, T.; Wang, T. T. *Macromolecules* **1975**, *8*, 909.
(13) Olabisi, O.; Robeson, L. M.; Shaw, M. T. *Polymer–Polymer Miscibility*; Academic: New York, 1979; Chapter 2.
(14) Flory, P. J. *Principles of Polymer Chemistry*; Cornell University Press: Ithaca, NY, 1953; p 509.
(15) Gryte, C. C.; Berghmans, H.; Smets, G. *J. Polym. Sci. Polym. Phys. Ed.* **1979**, *17*, 1295.
(16) Buckley, C. P.; Kovacs, A. J. *Colloid Polym. Sci.* **1976**, *254*, 695.
(17) Rhines, F. N. *Phase Diagrams in Metallurgy*; McGraw-Hill: New York, 1951; p 85.
(18) Robeson, L. M.; Hale, W. F.; Merriam, C. N. *Macromolecules* **1981**, *14*, 1644.
(19) Plester, D. W.; Rogers, S. E.; Ubbelohde, F. R. S. *Proc. R. Soc. London, A* **1956**, *235*, 469.
(20) Sakiyama, M.; Suga, H.; Seki, S. *Bull. Chem. Soc. Jpn.* **1963**, *36*, 1025.

Model Copolymerization Reactions. Determination of the Relative Rates of Addition of Styrene and Acrylonitrile to the 1-Cyanoethyl Radical

Glenn S. Prementine

Department of Chemistry, Carnegie-Mellon University, Pittsburgh, Pennsylvania 15213

David A. Tirrell*

Department of Polymer Science and Engineering, University of Massachusetts, Amherst, Massachusetts 01003. *Received April 13, 1987*

ABSTRACT: 2,2′-Azobis([2-^{13}C]propionitrile) (1) was prepared in 35% overall yield starting from [1-^{13}C]-acetaldehyde (99 atom %). Quantitative ^{13}C NMR analysis of end groups in styrene–acrylonitrile copolymers prepared with 1 as initiator allows determination of the relative rates of addition of these olefins to the 1-cyanoethyl radical. We have found $k_A/k_S = 0.12 \pm 0.03$, a result conistent with the penultimate model treatment of this copolymerization system by Hill, O'Donnell, and O'Sullivan.

Introduction

The development of a thorough understanding of the factors that control the structure of copolymer chains has been frustrated by a lack of analytical methodology capable of discriminating among alternative mechanistic proposals. Following the pioneering efforts of Mayo and Lewis,[1] Alfrey and Goldfinger,[2] and Wall,[3] early workers in the area of radical copolymerization found that their measurements

0024-9297/87/2220-3034$01.50/0